SANDIA REPORT

SAND 2016-xxxx
Unlimited Release
Printed January 2016

Numerical Estimation of the Spent Fuel Ratio

E.R. Lindgren, S.G. Durbin, J. Wilke, J. Margraf and T.A. Dunn

Prepared by
Sandia National Laboratories
Albuquerque, New Mexico 87185 and Livermore, California 94550

Sandia National Laboratories is a multi-program laboratory managed and operated by Sandia Corporation, a wholly owned subsidiary of Lockheed Martin Corporation, for the U.S. Department of Energy's National Nuclear Security Administration under contract DE-AC04-94AL85000.

Issued by Sandia National Laboratories, operated for the United States Department of Energy by Sandia Corporation.

Available to DOE and DOE contractors from
U.S. Department of Energy
Office of Scientific and Technical Information
P.O. Box 62
Oak Ridge, TN 37831

Telephone: (865) 576-8401
Facsimile: (865) 576-5728
E-Mail: reports@adonis.osti.gov
Online ordering: http://www.osti.gov/bridge

Available to the public from
U.S. Department of Commerce
National Technical Information Service
5285 Port Royal Rd.
Springfield, VA 22161

Telephone: (800) 553-6847
Facsimile: (703) 605-6900
E-Mail: orders@ntis.fedworld.gov
Online order: http://www.ntis.gov/help/order-methods/#online

SAND2016-0965
Unlimited Release
Printed January 2016

Numerical Estimation of the Spent Fuel Ratio

E.R. Lindgren, S.G. Durbin, and J. Wilke
Sandia National Laboratories
P.O. Box 5800
Albuquerque, New Mexico 87185-MS0747

J. Margraf and T.A. Dunn
Lawrence Livermore National Laboratory
7000 East Ave
Livermore, California 94550

Abstract

Sabotage of spent nuclear fuel casks remains a concern nearly forty years after attacks against shipment casks were first analyzed and has a renewed relevance in the post-9/11 environment. A limited number of full-scale tests and supporting efforts using surrogate materials, typically depleted uranium dioxide (DUO_2), have been conducted in the interim to more definitively determine the source term from these postulated events. However, the validity of these large-scale results remain in question due to the lack of a defensible spent fuel ratio (SFR), defined as the amount of respirable aerosol generated by an attack on a mass of spent fuel compared to that of an otherwise identical surrogate. Previous attempts to define the SFR in the 1980's have resulted in estimates ranging from 0.42 to 12 and include suboptimal experimental techniques and data comparisons. Because of the large uncertainty surrounding the SFR, estimates of releases from security-related events may be unnecessarily conservative. Credible arguments exist that the SFR does not exceed a value of unity. A defensible determination of the SFR in this lower range would greatly reduce the calculated risk associated with the transport and storage of spent nuclear fuel in dry cask systems.

In the present work, the shock physics codes CTH and ALE3D were used to simulate spent nuclear fuel (SNF) and DUO_2 targets impacted by a high-velocity jet at an ambient temperature condition. These preliminary results are used to illustrate an approach to estimate the respirable release fraction for each type of material and ultimately, an estimate of the SFR.

This page intentionally blank

TABLE OF CONTENTS

ABBREVIATIONS/DEFINITIONS VI

1 INTRODUCTION 1
1.1 Previous Attempts to Measure the SFR 1
1.2 Microstructural Changes in Irradiated Fuel 2

2 MODELING OF THE SPENT FUEL RATIO 3
2.1 Model Descriptions 3
2.2 Estimation of Respirable Fraction 5

3 PRELIMINARY RESULTS 7

4 SUMMARY 11

5 REFERENCES 13

FIGURES

Figure 2.1 Modeling domain in CTH. 4
Figure 2.2 Energy density at t = 2, 4, 8, and 16 μs. 4
Figure 2.3 Mass of aerosols with aerodynamic equivalent diameter (AED) < 10 μm normalized by affected mass as a function of energy density. 5
Figure 2.4 Mass of SNF and DUO2 aerosols with aerodynamic equivalent diameter (AED) < 10 μm normalized by affected mass as a function of energy density. 6
Figure 3.1 Internal energy density of the central pellet for different modeling cases. 8

TABLES

Table 3.1 Spent fuel ratio for all modeling cases. 9

ABBREVIATIONS/DEFINITIONS

AED	aerodynamic equivalent diameter
ALE	arbitrary Lagrangian-Eulerian
ALE3D	LLNL shock physics code
BCL	Battelle Columbus Laboratories
CTH	SNL shock physics code
DUO_2	depleted uranium oxide
EOS	equation of state
GRS	German Reactor Safety Authority
GWd	gigawatt-days
HED	high energy device
INL	Idaho National Laboratory
MTHM	metric ton heavy metal
NRC	Nuclear Regulatory Commission
OD	outer diameter
SFR	spent fuel ratio
SNF	spent nuclear fuel
SNL	Sandia National Laboratories
UO_2	uranium oxide

1 INTRODUCTION

A number of studies have been commissioned over four decades to estimate the source term and subsequent results of exposure from postulated attacks. In the late 1970's, a conservative analysis was published by Sandia National Laboratories (SNL) [DuCharme *et al.*, 1978]. Due to lack of experimental data, the study by DuCharme used expert judgment to define the amount of material released by an attack in downtown Manhattan. As a result the US Nuclear Regulatory Commission (NRC) imposed new regulations requiring increased security for shipments of spent fuel to protect against sabotage events.

In response to the perceived conservatisms in the report by DuCharme, a second analysis was conducted in an attempt to refine the assumptions made in the original assessment [Finley *et al*., 1980]. The estimated releases from this new study were 14 times lower than reported in the DuCharme report, but the NRC did not relax the interim regulations on the transportation of spent fuel at that time.

1.1 Previous Attempts to Measure the SFR

Acknowledging the lack of experimental data in this technical area, the NRC and DOE both funded parallel test programs to determine the source term from full-scale and scaled casks. The costs and safety requirements to conduct the full-scale tests with actual spent fuel would have been prohibitive. Therefore, the test planners at SNL chose to conduct the full-scale tests with fuel rods filled with surrogate pellets made of depleted uranium dioxide (DUO_2) [Sandoval *et al*., 1983]. DUO_2 was chosen in an attempt to best match the mechanical response of spent fuel interacting with a high energy device (HED). This substitution appears justified because spent fuel contains approximately 90% by mass of U-238 dioxide. However, actual spent fuel pellets contain several properties unique to irradiated fuel such as fission products, a fragmented structure, and embrittled cladding. The ability to scale the results of the full-scale sabotage tests for expected releases from actual spent fuel required the measurement of a spent fuel ratio (SFR). The SFR is defined as the ratio between the spent fuel respirable aerosol mass released to the DUO_2 surrogate respirable aerosol mass released under other otherwise identical, disruptive conditions. Respirable aerosols are defined as particles with an aerodynamic equivalent diameter (AED) less than 10 μm, which for UO_2 particles translates to a geometric diameter of 3.2 μm.

Subsequent large scale tests conducted by SNL and Gesellschaft für Anlagen- und Reaktorsicherheit (GRS, German Reactor Safety Authority) also elected to use DUO_2 as a fuel surrogate, further increasing the importance of the SFR for accurate source term interpretation [Philbin *et al*., 1988; Lange *et al*., 1994].

Two parallel programs, one at Battelle Columbus Laboratories (BCL) and another at Idaho National Engineering Laboratory (INL), were conducted in the early 1980's to obtain the SFR but resulted in inconclusive results [Schmidt *et al*., 1982; Alvarez *et al*., 1982]. A follow-on effort was conducted in the 2000's at SNL, but funding was discontinued prior to testing with spent fuel [Molecke *et al*., 2008].

1.2 Microstructural Changes in Irradiated Fuel

The ceramic density is a key material property needed to describe fresh fuel and SNF. The ceramic density throughout fresh fuel is initially uniform at between 95 to 96% of the theoretical maximum density of UO_2 (10.97 g/cm^3). During irradiation a number of physical phenomena change the fuel microstructure. Each fission event in the fuel produces two fission products. Some fission products are solids and others are gases. Both solid and gaseous fission products contribute to fuel swelling that reduces the fuel ceramic density. After an initial period of slight densification at low burnup (< 15 GWd/MTHM), the density of the fuel pellet decreases linearly with burnup [Caruso, 2007].

The grain size in fresh fuel is typically in the range of 10 to 20 μm [Noirot *et al.*, 2009]. As the fuel is irradiated to high burnup (> 60 GWd/MTHM), the grain size decreases significantly (~0.3 μm) concomitant with the formation of small (~0.5 μm) pores [Walker *et al*., 1992; Koo *et al*, 2001]. Calculated pore pressures in these small pores in high burnup fuel range from 100 to 500 MPa and are considered to be partly responsible for the pellet swelling [Koo *et al.*, 2001].

As stated previously, the UO_2 particles of interest have geometric diameters less than 3.2 μm. Ductile materials characteristically fracture along the grain boundaries (intergranular fracture). If high burnup SNF and surrogate materials were to behave as ductile materials, the small grain size of irradiated fuel would result in a greater release of respirable aerosols than the larger grained fresh fuel. This behavior would lead to a SFR significantly greater than unity. However, UO_2 behaves as a brittle material at temperatures below 1900 K, the brittle-ductile transition temperature [Cronenberg and Yackle, 1979]. Below 1900 K, fracture of the fuel pellets occurs through the grains (intragranular fracture) resulting in respirable aerosol release that is independent of grain size. An inherent assumption in the CTH modeling approach for this work is that the fracture characteristics of surrogate and irradiated fuel are similar and not dependent on grain size. The validity of this assumption is reviewed in the results section to verify that the fracture temperature is below the brittle-ductile transition temperature of 1900 K.

2 MODELING OF THE SPENT FUEL RATIO

2.1 Model Descriptions

The CTH and ALE3D hydrocodes were chosen to study the reaction of spent nuclear fuel (SNF) and DUO_2 under loadings imparted by an HED. CTH is an explicit Eulerian code developed by SNL for solving high strain transient dynamics problems including shaped charges, explosions, and high velocity impact problems. The code can be run in one, two, or three dimensions. CTH has a large internal library of equation of state (EOS) data, including SESAME and ANEOS tabular forms. These EOS libraries track heating, liquefaction, and vaporization of materials, as well as solid phase changes caused by high pressure. CTH allows the user to choose from a variety of constitutive models for strength and fracture or failure models. Also, developer models are available that allow the user to build custom constitutive models. The code will run on workstations or cluster computers using from one to over 100,000 processing cores in parallel. An adaptive mesh capability allows the user to select which components of a problem to finely resolve. CTH can read in a variety of geometry file formats and generates output data files that may be studied using several different post-processing and visualization codes.

ALE3D is a multi-physics numerical simulation software tool utilizing arbitrary Lagrangian-Eulerian (ALE) techniques. The code is written to address two-dimensional (2D) and three-dimensional (3D) physics and engineering problems using a hybrid finite element and finite volume formulation on an unstructured grid. The ALE and mesh relaxation capability broadens the scope of applications in comparison to tools restricted to Lagrangian-only or Eulerian-only approaches, while maintaining accuracy and efficiency for large, multi-physics and complex geometry simulations. Beyond its foundation as a hydrodynamics and structures code, ALE3D has multi-physics capabilities that integrate various packages through an operator-splitting approach. Additional ALE3D features include heat conduction, chemical kinetics and species diffusion, incompressible flow, a wide range of material models, chemistry models, multi-phase flow, and magneto-hydrodynamics for long (implicit) to short (explicit) time-scale applications.

The CTH modeling domain simulating an ambient temperature experiment is shown in Figure 2.1 and includes small dishes between pellets. For these preliminary calculations the CSC jet is represented by a copper cylinder 20 mm long by 2 mm diameter with a velocity of 7.8 km/s and is depicted to the left of the target. The target is centered in the domain and is composed of a stack of seven UO_2 pellets each 15.2 mm tall and 9.3 mm diameter inside of a 10.7 mm OD Zircaloy tube with 0.62 mm wall thickness. The initial density of the surrogate DUO_2 was set to 10.49 g/cc for these calculations. The copper jet strikes the middle of the center pellet in the model. The ALE3D modeling domain is essentially the same as shown in Figure 2.1 except the dish detail was not included. Figure 2.2 shows energy density as the jet strikes the target at 2, 4, 8, and 16 μs. Nearly all of the energy of the rod is deposited in the center pellet.

The material properties of spent fuel are studied by parametrically modifying the DUO_2 properties. The effect of density was explored in these preliminary calculations by reducing the initial density of fresh DUO_2 fuel from 10.49 to 9.87 g/cc using both CTH and ALE3D. For these simulations the fuel pellet material is assumed to be non-porous with a uniform density. The effect of increased brittleness, which is characteristic of SNF, was also investigated with CTH by changing the failure strain in the constitutive model from 8% to 4%.

In a separate treatment, the surrogate and spent fuel pellets were treated as a porous material with a P-alpha model with effective densities of 10.49, 10.14, 10.02 and 9.87 g/cc (corresponding to fuel burnup of zero and approximately 45, 60 and 80 GWd/MTHM, respectively). This porous material must first undergo compaction of the pore space before undergoing compression of the solid component along the Hugoniot curve, which describes the material pressure as a function of specific volume. The Rankine-Hugoniot jump equations relationships are used to relate pressure and density to particle velocity and shock velocity. The compaction of the porous material was treated using the P-alpha model. For the P-alpha model, the user specifies a porous density, initial porous crush pressure, and a final crush pressure required to compact the foam to a solid material. After this point, the material is again modeled as a solid using the Mie-Grunieson EOS. For these preliminary simulations, the initial crush pressure and final crush pressure were assumed to be 1034 and 3447 MPa, respectively.

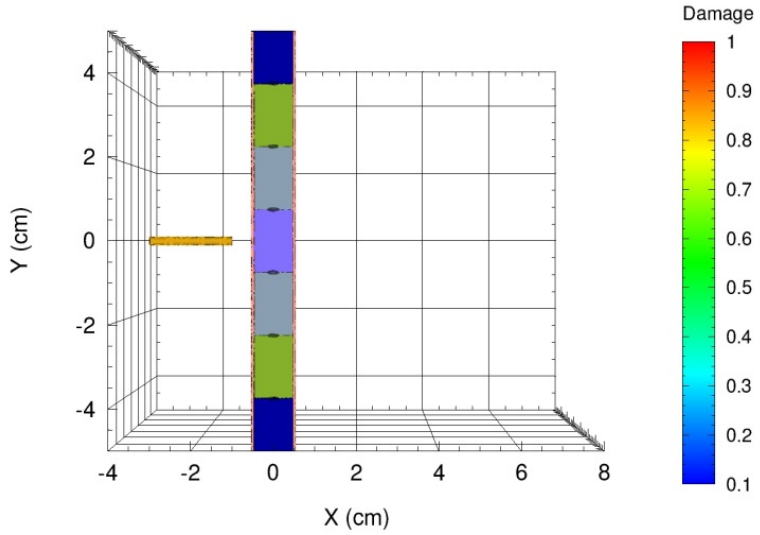

Figure 2.1 Modeling domain in CTH.

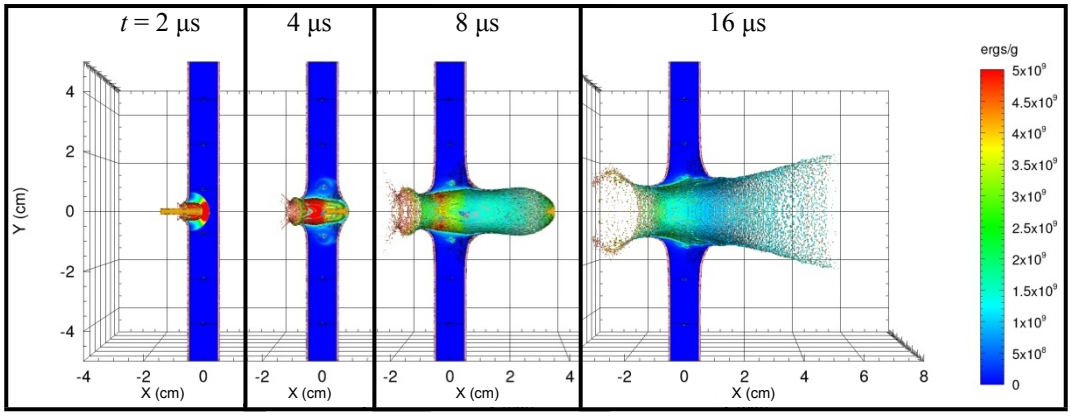

Figure 2.2 Energy density at t = 2, 4, 8, and 16 µs.

2.2 Estimation of Respirable Fraction

The numerical simulations do not need to directly determine the particle size distribution produced by the interaction. Previous studies have postulated that the respirable release fraction is a function of energy density such as shown in Figure 2.3, where the respirable release fraction is assumed to be particles equal to or smaller than 10 µm aerodynamic equivalent diameter (AED) [Durbin and Luna, 2013]. The data represented in Figure 2.3 are taken from various sources and include glasses, vitrified waste forms, DUO_2, and limited samples of SNF [Alvarez *et al*., 1982; Molecke *et al*., 2008; Jardine *et al*., 1982; Ruhmann *et al*., 1985]. The burnup of the SNF samples is shown in gigawatt-days per metric ton of heavy metal (GWd/MTHM).

For these studies the data of most interest are those for DUO_2 and SNF. These data are replotted and fitted in Figure 2.4. From this relationship the respirable release fraction generated by a disrupted pellet can be calculated from the energy density imparted to the pellet.

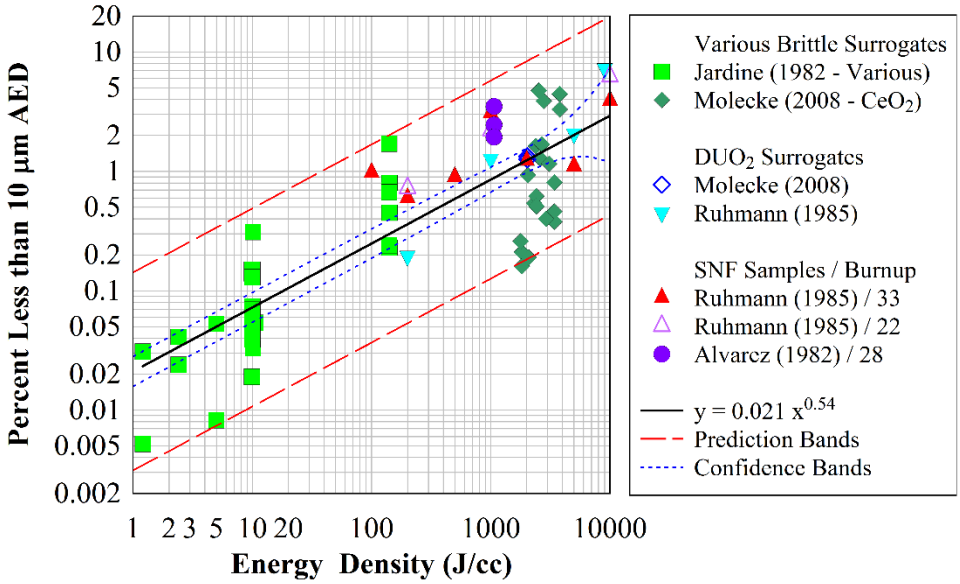

Figure 2.3 Mass of aerosols with aerodynamic equivalent diameter (AED) < 10 µm normalized by affected mass as a function of energy density.

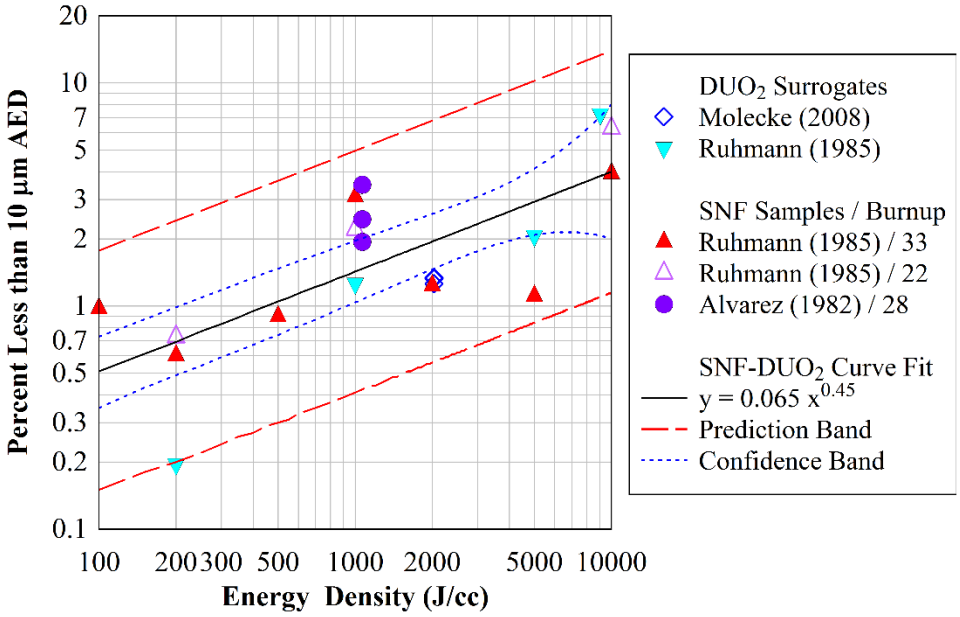

Figure 2.4 Mass of SNF and DUO2 aerosols with aerodynamic equivalent diameter (AED) < 10 µm normalized by affected mass as a function of energy density.

3 PRELIMINARY RESULTS

The increase in internal energy density of the middle pellet was used to estimate the respirable release fraction. Figure 3.1 shows the internal energy increase with time for the base cases (DUO_2) and several simulated SNF materials for the two density treatments considered. The inset pictures show the CTH derived energy density distribution of the copper jet interaction with the fuel pellet at the time indicated. The initial sharp peak in internal energy is due to high pressures associated with the passage of the shock wave through the pellet. This energy is imparted into the pellet because the material follows the Rayleigh jump line at the shock front and then the pressure-volume Hugoniot line during subsequent pressure decay. The Rayleigh line and Hugoniot enclose an area in the pressure-volume Hugoniot plane, which corresponds to the imparted energy.

Both CTH and ALE3D were used to evaluate the uniform density sensitivity cases. The pellet initial density was decreased in the Mie-Gruneisen EOS from 10.49 g/cc which represents fresh fuel to 9.87 g/cc which represents 80 GWd/MTHM spent fuel. The two codes are in good agreement over the initial 4 μs. The initial energy density peak is reached in about 2.5 μs. At this point the copper jet is about mid-way through the pellet. The initial peak for the ALE3D simulation is 40 J/cc higher that for the corresponding CTH simulation. The initial peak for the 9.87 g/cc spent fuel CTH simulation is 50 J/cc lower than the 10.49 g/cc fresh fuel CTH simulation. At about 4 μs the jet is just breaking through the back side of the pellet. After 4 μs the results from the two codes begin to deviate. While both codes show an increase in the energy density the increase by CTH is more pronounced. The reason for this difference is still under investigation. By 15 μs the copper jet has exited the calculation domain. Both codes show that the final energy density plateau is lower for pellets with density of 9.87 g/cc than those corresponding to fresh fuel. The difference in the energy density is 50 J/cc for CTH and 10 J/cc for ALE3D.

The failure strain was reduced by a factor of two in CTH for a brittle sensitivity case (not shown). This reduction in ductility resulted in negligible 10 J/cc reduction in the plateau internal energy density. The changes in initial uniform density and fuel ductility explored in this preliminary study did not have a significant effect on the energy imparted to the target material.

The largest increase in energy density was realized by reducing the pellet density using the P-alpha model in CTH. Treating the ceramic as a crushable, porous material increases the internal energy of the target material while reducing its kinetic energy. This is because work is performed on the material as the pore space is compacted. Based on a theoretical density of 10.97 g/cc for UO_2 ceramic, four fuel pellets ranging from fresh fuel with a density of 10.49 g/cc to 80 GWd/MTHM spent fuel with a density of 9.87 g/cc were studied. As shown in Figure 3.1 both the initial peak energy density and the final plateau energy density for all cases increased noticeably compared to the uniform density cases. As the density decreased the energy density increased. However, these results for crushable SNF are preliminary as the parameters currently used in the P-alpha model have not yet been validated for spent fuel. Efforts are underway to corroborate these results using ALE3D.

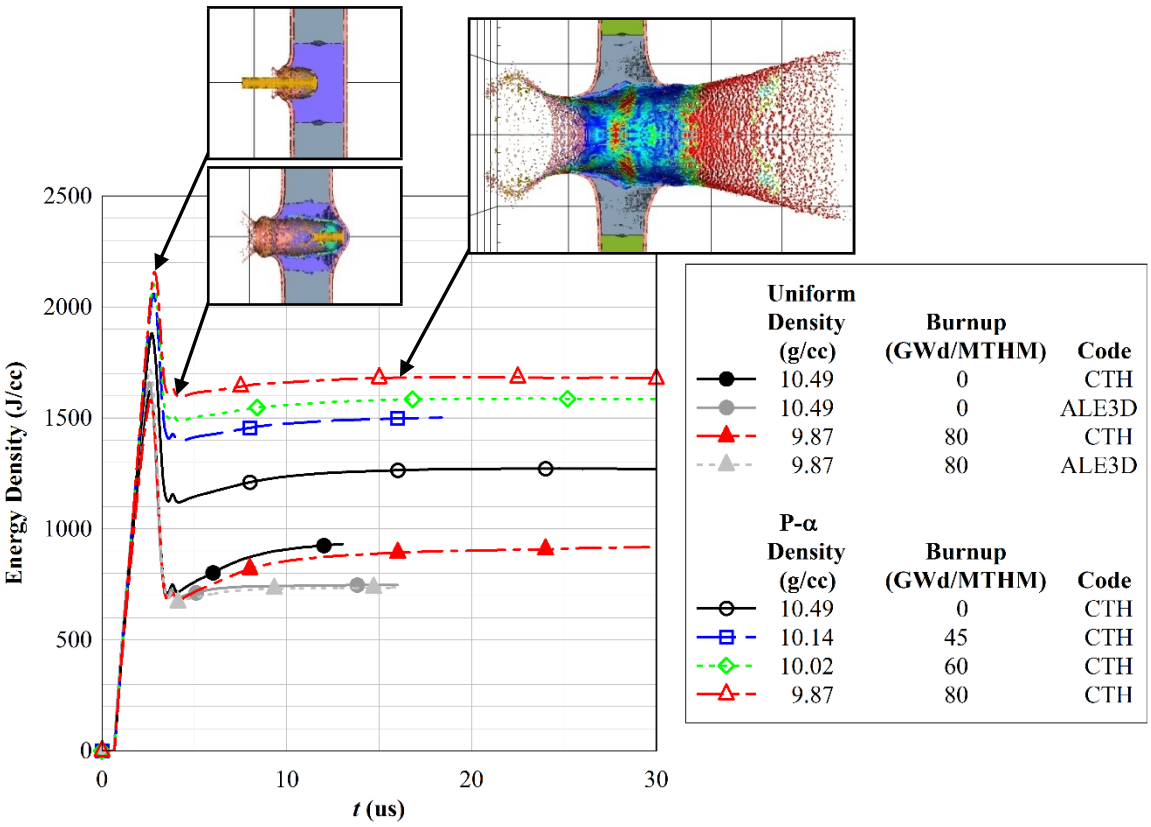

Figure 3.1 Internal energy density of the central pellet for different modeling cases.

Table 3.1summarizes the results for all modeling cases in this study. The listed energy density is the maximum of the final plateau typically found in the range of 15 to 30 μs. The percent respirable release (< 10 μm AED) is calculated from the energy density using the curve fit in Figure 2.4. The SFR was calculated by dividing the respirable percentage for the irradiated cases (burnup > 0) by the respirable percentage from the DUO_2 case (zero burnup).

For the uniform density cases, ALE3D generally calculates a lower energy density than calculated by CTH. As a result the respirable release of 1.3% determined by the ALE3D results is slightly lower than the respirable release of 1.4% determined by the CTH results. However, the resulting SFR is the same at 1.0, even though the respirable releases differ.

The largest changes to energy density were observed for the cases using the porous P-alpha model. The energy density for all porous cases is higher than the uniform density cases. For the zero burnup fresh fuel the release fraction base case is 1.6%. As the spent fuel burnup increases, the energy density and respirable release increases. However, the SFR for all porous density cases is determined to be the same at 1.1. These results should be considered preliminary. A broader treatment of the parameter space is underway, and assumptions in the material characteristics still require validation. However, these early results indicate that arguments for an SFR approaching unity appear to be justified.

Table 3.1 Spent fuel ratio for all modeling cases.

Code	Density (g/cc)	Burnup (GWd/MTHM	Energy Density (J/cc)	Resp. (%)	SFR
Uniform Density Cases					
ALE3D	10.49	0	750	1.3	--
CTH	10.49	0	930	1.4	--
CTH	9.87	80	880	1.4	1.0
ALE3D	9.87	80	740	1.3	1.0
Porous Cases (P-α)					
CTH	10.49	0	1270	1.6	--
CTH	10.14	45	1500	1.7	1.1
CTH	10.02	60	1590	1.8	1.1
CTH	9.87	80	1680	1.8	1.1

The average temperature of the pellet during fracture can be estimated from the energy density, thermal mass, and initial temperature of the pellet. The initial temperature for the simulations shown here is 298 K, which models an ambient temperature experiment. The average $\rho \cdot C_p$ of 9.87 g/cc UO_2 between 298 K and 900 K is 2.78 J/(cc·K), which would result in a temperature increase of about 600 K for the highest calculated energy density of 1680 J/cc [Popov *et al.*, 2000]. Therefore, the estimated temperature during fracture is 900 K, which is well below the 1900 K brittle-ductile transition temperature [Cronenberg and Yackle, 1979]. Again, fractures below this transition temperature are dominated by intragranular breakup and provide a plausible mechanism by which SNF and DUO_2 surrogates may be characterized by similar respirable releases.

This argument also extends to SNF should this type of fracture occur under storage conditions. In this situation, a conservative upper limit of the temperature of a fuel pellet in dry storage is 673 K. The average fracture temperature for SNF would then be 1250 K, which is still well below the transition temperature.

This page intentionally blank

4 SUMMARY

A modeling and simulation effort was commenced to explore the determination of a defensible SFR using two shock physics codes, CTH and ALE3D. These efforts combine the capabilities of the shock-physics codes with the available empirical data for respirable particle production of DUO_2 and SNF samples under high-energy loadings. For a uniform density case both codes determined the SFR to equal unity. The largest changes to energy density were observed for the cases using the porous P-alpha model in CTH. The energy density for all porous cases is higher than the uniform density cases but the SFR only increases to 1.1.

Preliminary results presented in this paper indicate that an SFR of unity appears to be justified. However, additional studies are ongoing that will investigate a wider set of mechanical properties for simulated SNF. In addition, treatments of material characteristics in the P-alpha model require validation. Other, porous models may also be evaluated in future work. Additionally the effect of radial distribution of porosity in the spent fuel pellet will also be considered.

This page intentionally blank

5 REFERENCES

Alvarez J. L. *et al.*, "Waste Forms Project: Correlation Testing", Idaho National Engineering Laboratory Report EGG-PR-5590, (1982).

Caruso, S "Characterisation of High-Burnup LWR Fuel Rods through Gamma Tomography", PhD Thesis No. 3762, École Polytechnique Federale de Lausanne (EPFL), Switzerland, (2007).

Cronenberg, A. W. and T. R. Yackle, "Intergranular Fracture of Unrestricted UO_2 Fuel during Film-Boiling Operation," *J. Nucl. Mater.*, **84**, 295-318 (1979).

Ducharme, A. R. *et al.*, "Transportation of Radionuclides in Urban Environs: Working Draft Assessment," Sandia National Laboratories, Report SAND77-1927, (1978).

Durbin, S. G. and R. E. Luna, "A Methodology to Quantify the Release of Spent Nuclear Fuel from Dry Casks during Security-Related Scenarios," Sandia National Laboratories, SAND2013-9684, (2013).

Finley, N. C. *et al.*,, Transportation of Radionuclides in Urban Environs: Draft Environmental Assessment," Nuclear Regulatory Commission, NUREG/CR-2472, (1980).

Jardine, L. J. *et al.*, "Final Report of Experimental Laboratory Scale Brittle Fracture Studies of Glasses and Ceramics," Argonne National Laboratory, Report ANL-82-39, (1982).

Koo, Y. H., B. H. Lee, J. S. Cheon, and D. S. Sohn, "Pore Pressure and Swelling in the Rim Region of LWR High Burnup UO_2 Fuel," *J. Nucl. Mater.*, **295**, 213-220, (2001).

Lange, F. *et al.*, "Experimental Determination for UO_2 Release from a Spent Fuel Transport Cask after Shaped Charge Attack," Proc. INMM 35th Meeting, Naples, Florida, July 17-20, (1994).

Molecke, M. A. *et al.*, "Spent Fuel Sabotage Test Program, Characterization of Aerosol Dispersal: Interim Final Report", Sandia National Laboratories, Report SAND2007-8070, (2008).

Noirot, J. *et al.*, "High Burnup Changes in UO_2 Fuels Irradiated up to 83 GWD/T in M5® Claddings", *Nucl. Eng. Technol.*, **41** NO. 2, Special Issue on the Water Reactor Fuel Performance Meeting, (2009).

Philbin, J. S. *et al.*, "Behavior of a Simulated, Metal Spent-Fuel Storage Cask under Explosive Attack," Sandia National Laboratories, Report SAND87-2358C, (1988).

Popov, S.G., V. K. Ivanov, J. J. Carbajo and G. L. Yoder, "Thermophysical Properties of MOX and UO_2 Fuels Including the Effects of Irradiation," ORNL/TM-2000/351, (2000).

Ruhmann, H. *et al.*, "Research Program on the Behavior of Burnt-Up Fuel under Strong Mechanical Impacts," Kraftwerk Union, Report R 917/85/002, (1985).

Sandoval, R. P. *et al.*, "An Assessment of the Safety of Spent Fuel Transportation in Urban Environs", Sandia National Laboratories, Report SAND82-2365, (1983).

Schmidt, E. W. *et al.*, "Final Report on Shipping Cask Sabotage Source Term Investigation," BMI-2095, NUREG/CR-2472, Battelle Columbus Laboratory, Columbus, OH, (1982).

Walker, C. T. *et al.*, "Concerning the Microstructure Changes that Occur at the Surface of UO_2 Pellets on Irradiation to High Burnup", *J. Nucl. Mater.*, **188**, 73-79, (1992).

DISTRIBUTION

Sandia Internal:

6223	MS0747	Samuel Durbin (3)
6223	MS0747	Eric Lindgren
6223	MS0747	Ken Sorenson
6626	MS0783	Jason Wilke
9532	MS0899	Technical Library (electronic copy)


Sandia National Laboratories